Trifluoroethanol Promotes Helix Formation by Destabilizing Backbone Exposure: Desolvation Rather than Native Hydrogen Bonding Defines the Kinetic Pathway of Dimeric Coiled Coil Folding†

Alex Kentsis and Tobin R. Sosnick*

Department of Biochemistry and Molecular Biology, University of Chicago, 920 East 58th Street, Chicago, Illinois 60637

Received July 9, 1998

ABSTRACT: We measure the effects of low concentrations of helix-stabilizing cosolvents, including 2,2,2-trifluoroethanol (TFE), on the thermodynamics and kinetics of folding of the dimeric α-helical coiled coil derived from the leucine zipper region of bZIP transcriptional activator GCN4. The change in kinetic behavior upon addition of 5% (v/v) TFE indicates that it stabilizes the transition state to the same degree as the fully helical native state. However, folding rates are largely insensitive to alanine to glycine mutagenesis, indicating that the majority of helical structure is formed after the transition state. Equilibrium hydrogen isotope partitioning measurements indicate that intramolecular hydrogen bonds are not strengthened by TFE and that amide hydrogen bonds in the transition state are nearly the same strength as those in the unfolded state. Thus, the mechanism by which TFE exerts its helix-stabilizing effects can be divorced from helix formation and does not depend on the strengthening of intrahelical hydrogen bonds. Rather, TFE increases the structure of the binary alcohol/water solvent, thereby increasing the energetic cost associated with solvation of the polypeptide backbone. At low concentrations, TFE destabilizes the unfolded species and thereby indirectly enhances the kinetics and thermodynamics of folding of the coiled coil. A high degree of polypeptide backbone desolvation, and not the formation of regular helical structure and native strength hydrogen bonds, is the critical feature of the transition state for folding of this small dimeric protein.

The structure and stability of proteins exist in a delicate balance between the stabilizing interactions of the folded chain with itself and the destabilizing interactions of the unfolded polypeptide with its solvent environment. Proteins exhibit dramatically different folding behavior when observed in vacuo (*1*, *2*), and short polypeptide segments generally fail to adopt stable conformations (*1*). To overcome the shortage of native intramolecular interactions and to identify intrinsic structural preferences, protein segments are often studied in the presence of stabilizing cosolvents. For example, the ability of monohydric alcohols, particularly 2,2,2-trifluoroethanol (TFE[1]), to enhance helix formation has become a frequently used tool in equilibrium (*2*−*4*) and kinetic protein folding studies (*5*, *6*). At high concentrations, this cosolvent partially denatures proteins by destabilizing tertiary architectures, while preserving secondary organization (*4*, *7*, *8*), presumably due to the apolar character of its trifluoroethyl surface (*9*, *10*). At low concentrations, TFE enhances the helicity of short polypeptides, the magnitude of this effect being correlated with the α-helical propensity of the amino acid sequence (*3*). Despite TFE's widespread usage, its helix-inducing mechanism remains unclear. Some work has noted that TFE may stabilize the folded state (*2*, *3*), possibly by explicitly strengthening intramolecular hydrogen bonding (*11*). Alternatively, TFE may increase the free energy of the unfolded state (*12*−*14*), producing a thermodynamically equivalent effect of native state stabilization, but doing so indirectly.

We sought to examine the mechanism of helix induction by monohydric alcohols and, with this knowledge, to use low concentrations of these cosolvents as a heuristic probe to investigate the folding pathway of a structurally uncomplicated and rapidly folding α-helical coiled coil. Ideally, TFE's helix-inducing ability would enable us to resolve an uncertainty in our previous studies of the folding of this 33-residue dimeric coiled coil derived from the leucine zipper region of bZIP transcriptional activator GCN4 (*15*). Refolding rates of GCN4-p1′ were largely insensitive to single-site helix-destabilizing substitutions (alanine to glycine) down the length of the coiled coil, indicating that minimal helical structure is present in the transition state at each of the individually substituted sites. To probe the total helicity of all sites simultaneously, and quantify the total helical content of the transition state, the coiled coil was refolded in the presence of TFE at low concentrations. Given the earlier results of Ala to Gly mutagenesis (*15*) and TFE's ability to stabilize α-helical structures, we expected TFE to have a minimal effect on the refolding kinetics.

† Supported in part by a HHMI Undergraduate Education Initiative Grant to the University of Chicago (A.K.) and NIH Research Grant GM55694 (T.R.S.).

* To whom correspondence should be addressed. Telephone: (773) 834-0657. Fax: (773) 702-0439. E-mail: trsosnic@midway.uchicago.edu.

[1] Abbreviations: CD, circular dichroism; EtOH, ethanol; GdmHCl, guanidinium hydrochloride; HX, hydrogen exchange; MeOH, methanol; TFE, 2,2,2-trifluoroethanol.

S0006-2960(98)01641-9 CCC: $15.00
Published on Web 09/25/1998

Surprisingly, TFE exhibits its entire stabilizing effect by enhancing refolding rates, indicating that native and transition states are equivalently stabilized, and suggesting that the latter is fully helical. However, a simultaneous triple alanine to glycine substitution (total of six in the dimer) exhibits nearly the same kinetic effect as the single-site comparisons, even in 5% TFE, thereby discounting the possibility that the transition state is helical to a major degree (L. Moran, J. Schneider, A. Kentsis, and T. R. Sosnick, unpublished results). In this fashion, the stabilizing effect of TFE can be manifested on nonhelical structures. To advance this understanding, we directly examine the effect of TFE on hydrogen bond strength using equilibrium D−H isotope partitioning (*16*−*18*) and observe that TFE does not directly strengthen native intramolecular hydrogen bonds. Similarly, the insensitivity of folding rates to hydrogen isotope replacement indicates that the transition state hydrogen bonds are of nearly the same strength as those in the unfolded state. From these data as well as from the analysis of the folding reaction coordinate, we conclude that at low concentrations TFE and other monohydric alcohols act by a kosmotropic mechanism which promotes desolvation of the polypeptide backbone, instead of directly strengthening hydrogen bonds or stabilizing helical structures. Thus, in the fast folding of this small dimeric protein, a high degree of polypeptide backbone desolvation, and not formation of regular helical structure and native strength hydrogen bonds, is the critical feature of the folding transition state.

EXPERIMENTAL PROCEDURES

Chemicals. Ultrapure guanidinium hydrochloride (GdmHCl) was obtained from ICN Biomedicals (Aurora, OH), and concentrations were determined by refractometry. Deuterium oxide was purchased from Isotec (Miamisburg, OH). Tris(2-carboxyethyl)phosphine hydrochloride (phosphine) was obtained from Pierce (Rockford, IL). All other chemicals were purchased from Fisher Scientific (Fair Lawn, NJ).

Peptide Synthesis. Variants of the GCN4-p1′ polypeptide were prepared and characterized as in Choma et al. (*19*). To enable kinetic and equilibrium folding reactions to be monitored by fluorescence spectroscopy, we introduced the conservative substitution of a tryptophan for tyrosine 17 (GCN4-p1′, Ac-RMKQLEDKVEELLSKNWHLHLENEVARLKKLVGER-NH_2). A monomeric version of the coiled coil was created by adding an amino-terminal Cys-Gly-Gly disulfide-bonded cross-linker (GCN4-p2′). Protein concentrations were determined under denaturing conditions using an extinction coefficient for tryptophan at 280 nm of 5700 M^{-1} cm^{-1} (*20*).

Equilibrium Denaturation Measurements. Equilibrium values of the folding free energy, $\Delta G°$, for variants of GCN4-p1′ in 20−100 mM sodium acetate at pH 5.5 and 10 °C were determined with circular dichroism (CD). Denaturation measurements were conducted with a Jasco 715 spectrometer (Tokyo, Japan) at 222 nm (Θ_{222}), with 2 nm bandwidth, utilizing 10 mm wide quartz cuvettes having path lengths between 1 and 10 mm. The protein concentration ranged from 12 to 15 μM. For the dimeric version of the coiled coil, the thermodynamic parameters were obtained assuming a two-state equilibrium between unfolded monomers and folded dimers, and a linear dependence of $\Delta G°$ on GdmHCl concentration:

$$\Delta G°([\mathrm{GdmHCl}]) = -RT \ln K_U([\mathrm{GdmHCl}]) = \Delta G°_{H_2O} - m°[\mathrm{GdmHCl}] \quad (1)$$

where K_U is the equilibrium constant and the slope $m°$ is a measure of the denaturant-sensitive surface area exposed upon unfolding. The observed signal, Θ_{222}, was fit to

$$\Theta_{222} = F_N + \frac{F_N - F_U}{4\exp(Z)} - \frac{F_N - F_U}{4\sqrt{\exp(2Z) + 8\exp(Z)}} \quad (2)$$

where $Z = (-\Delta G° + m°[\mathrm{GdmHCl}])/RT$ and F_N and F_U are the baseline values of the folded and unfolded protein, respectively. The equilibrium dimerization constant, K_d, between folded dimers and unfolded monomers of dimeric GCN4-p2′ in 20−100 mM sodium acetate at pH 4.55 and 10 °C was determined using CD spectroscopy, and the peptide concentration-dependent Θ_{222} signal was fit to

$$\Theta_{222} = F_U x - F_U \frac{-1 + \sqrt{1 + 8K_d x}}{8K_d} + (F_N - F_U)/2 \quad (3)$$

where F_N and F_U are the baseline values for the dimeric and monomeric species, respectively, and x is the protein concentration.

Thermodynamic parameters of the monomeric version of the coiled coil GCN4-p2′ were obtained using

$$\Theta_{222} = F_N + m_f[\mathrm{GdmHCl}] + \frac{(F_U + m_u[\mathrm{GdmHCl}])\exp(Z)}{1 + \exp(Z)} \quad (4)$$

where m_f and m_u are the slopes of the baselines for the folded and unfolded states, respectively, and Z is the parameter defined in eq 2.

Stopped-Flow Spectroscopy. For rapid mixing fluorescence experiments, we used either a Biologic (Grenoble, France) SFM-3 or SFM-4 stopped-flow apparatus. The SFM-3 apparatus was equipped with a 200 W argon/mercury lamp and a TC/10 sample cuvette having a 10 mm path length and 1 mm width. The SFM-4 apparatus was interfaced with a Jasco model 715 CD spectropolarimeter and utilized a 0.8 mm × 0.8 mm square FC/08 cuvette. For fluorescence spectroscopy, we used excitation and emission wavelengths of 280−290 and 300−400 nm, respectively. The temperature of the sample syringes and the observation cuvette was maintained using a circulating water bath. The dead time of the stopped-flow measurements was 1−2 ms depending upon syringe speed and dilution ratio.

If they were started from the fully unfolded state (4−6 M GdmHCl) or the folded state (0−1 M GdmHCl), folding or refolding reactions were initiated by dilution to yield the desired denaturant concentration with 20−100 mM sodium acetate at pH 5.5 and 10 °C. Protein concentrations ranged from 2 to 12.5 μM. Two to six time courses were averaged under each reaction condition.

Kinetic data were analyzed using a Simplex algorithm as implemented in the Biologic Biokine software. The unfold-

ing data were fit to a single-exponential function and refolding data to a function describing a second-order bimolecular process to account for the dependence of refolding rates on polypeptide concentration.

Equilibrium Hydrogen Exchange Measurements. A 10-fold molar excess of phosphine hydrochloride was used to reduce disulfide-linked GCN4-p2′ and render it dimeric. Equilibrium values for the deuterium to protium backbone substitution, ΔG°_{D-H}, for the reduced dimeric form of GCN4-p2′ in 20−100 mM sodium acetate at pH 4.55 and 10 °C were determined by monitoring the change in protein stability, reflected in a change in Θ_{222}, as a function of the extent of backbone hydrogen exchange. Fully denatured and deuterated dimeric GCN4-p2′ in 6 M GdmDCl and D_2O (estimated D content of >98%) was manually diluted 100-fold into H_2O buffer at pH 4.55 and 10 °C to a final concentration close to its K_d value, where half of the molecules are unfolded. To test whether the experiment was conducted at the midpoint of the concentration-dependent folding transition, observed hydrogen exchange (HX) kinetics were compared to that expected for a population composed of 50% unfolded molecules. The predicted HX trace of this population was calculated as a sum of the individual exponential decays for each amide proton, accounting for the sequence dependence of amide HX rates (*21*).

Equilibrium Isotope Partitioning in Folding Kinetics. Kinetics of protonated and deuterated GCN4-p1′ were monitored using stopped-flow spectroscopy at pH 4.55 and 10 °C in the presence of 20 mM sodium acetate, 12% (v/v) D_2O, and varying amounts of GdmHCl. Kinetic measurements of fully protonated GCN4-p1′ were taken as described above. Refolding and unfolding rates of fully deuterated GCN4-p1′ were obtained by diluting the protein 8.3-fold from 100% D_2O buffer in the presence of varying amounts of GdmHCl to a final bulk solvent condition of 12% D_2O. This protocol was chosen so the effects of varying bulk solvent could be eliminated so that only the equilibrium effect of amide D−H substitution would be observed. In kinetic folding measurements of both deuterated and protonated GCN4-p1′, the potential effect of amide hydrogen exchange on the observed kinetics was overcome by carrying out the experiments at pH 4.55 where the rate of amide hydrogen exchange is 2−3 orders of magnitude slower than the observed refolding and unfolding kinetics.

RESULTS

Folding in the Presence of Cosolvents. The equilibrium stability of a Ser14Ala variant of the dimeric coiled coil, GCN4-p1′, is measured using CD at 222 nm (Θ_{222}, helix formation) in the presence of 5% (v/v) methanol (MetOH), 5% ethanol (EtOH), 5% TFE, and 0.5 M sodium sulfate. The guanidine denaturation profiles are consistent with the equilibrium transition being between α-helical dimers and fully unfolded monomers (*15*, *22*) (Figure 1). The ellipticity at 222 nm of the unfolded state remains essentially zero in the presence of all cosolvents, indicating that the monomer still completely denatures to the random coil state. In the presence of 5% MetOH, 5% EtOH, 5% TFE, and 0.5 M sodium sulfate, the folding free energy in zero denaturant, $\Delta G^{\circ}_{H_2O}$, increased by 1.2, 1.1, 1.7, and 1.6 kcal/mol, respectively (Table 1).

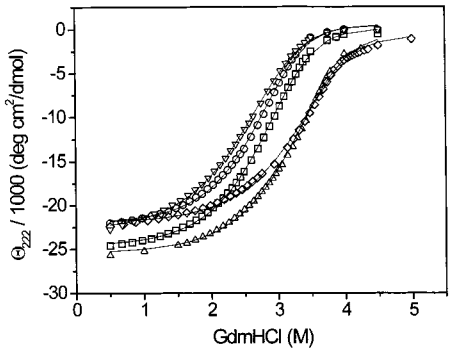

FIGURE 1: Equilibrium unfolding. Chemical denaturation profile of the Ser14Ala variant of GCN4-p1′ followed by CD at 222 nm in 20−100 mM sodium acetate at pH 5.5 and 10 °C (▽), and in the presence of 5% TFE (◇), 5% MetOH (□), 5% EtOH (△), and 0.5 M sodium sulfate (○).

Stopped-flow fluorescence spectroscopy is used to investigate the cosolvents' effects on the folding kinetics of the tryptophan-containing GCN4-p1′. When the monomeric random coil form of GCN4-p1′ in GdmHCl is diluted with aqueous buffer, a helical homodimer forms and the tryptophan 17 fluorescence intensity increases by approximately 50%. The second-order folding and first-order unfolding reactions of the dimeric coiled coil are well-described by a two-state bimolecular reaction between unfolded monomers and fully folded dimers (*15*, *22*):

$$2 \text{ monomers} \underset{k_u}{\overset{k_f}{\rightleftharpoons}} \text{dimer} \qquad (5)$$

The two-state nature of the reaction is rigorously validated by the equivalence of the equilibrium and kinetically determined values for the folding free energy and its denaturant dependence using the "chevron analysis" (*23*, *24*). The denaturant dependence of kinetic folding and unfolding reactions produces a chevron or V-shaped curve with its vertex at the midpoint of the equilibrium transition (Figure 2). The protein dependence of the unfolding equilibrium constant, K_U, and stability, ΔG°, on the concentration of GdmHCl is commonly described by the linear relationship shown in eq 1 where the slope m° is a measure of the denaturant-sensitive surface area exposed upon unfolding (*25*). Equations 6a and 6b describe the analogous linear dependence of the activation free energy, $\Delta G^{\ddagger}$, for kinetic folding (f) and unfolding (u) reactions

$$\Delta G_f^{\ddagger}([\text{GdmHCl}]) = -RT \ln k_f^{H_2O} - m_f[\text{GdmHCl}] + \text{constant} \qquad (6a)$$

$$\Delta G_u^{\ddagger}([\text{GdmHCl}]) = -RT \ln 2k_u^{H_2O} - m_u[\text{GdmHCl}] + \text{constant} \qquad (6b)$$

where $-m_f$ and m_u are proportional to the denaturant-sensitive surface area exposed on going from the initial state to the transition state. The slopes of the left and right limbs of the chevron represent these kinetic surface exposure parameters.

When equilibrium and kinetic folding reactions are effectively two-state, and are limited by the same activation barrier, the equilibrium values for the change in free energy and surface burial can be calculated from kinetic measurements according to $\Delta G^{\circ}_{H_2O} = -RT \ln K_u^{H_2O} = -RT \ln(2k_u^{H_2O}/$

Table 1: Equilibrium and Kinetic Parameters of GCN4-p1′ Folding in the Presence of Cosolvents[a]

	equilibrium		kinetic					
	$\Delta G°$ (kcal/mol)	$m°$ (kcal mol^{-1} M^{-1})	$\Delta G°$ (kcal/mol)	$-m_f$ (kcal mol^{-1} M^{-1})	m_u (kcal mol^{-1} M^{-1})	$m° = m_u - m_f$ (kcal mol^{-1} M^{-1})	k_f (s^{-1})	k_u (s^{-1})
aqueous buffer	-10.86 ± 0.09	1.78 ± 0.03	-10.78 ± 0.23	1.22 ± 0.15	0.55 ± 0.04	1.77 ± 0.16	4.96 ± 1.5	0.0101 ± 0.003
5% MetOH	-12.01 ± 0.10	2.09 ± 0.04	-11.70 ± 0.94	1.41 ± 0.20	0.66 ± 0.07	2.07 ± 0.21	31.66 ± 5.4	0.0133 ± 0.007
5% EtOH	-11.91 ± 0.08	1.99 ± 0.02	-11.81 ± 0.82	1.36 ± 0.28	0.70 ± 0.05	2.06 ± 0.28	28.29 ± 4.3	0.0100 ± 0.009
5% TFE	-12.51 ± 0.10	1.90 ± 0.05	-11.80 ± 1.7	1.18 ± 0.15	0.68 ± 0.12	1.86 ± 0.13	181.82 ± 21	0.008 ± 0.001
0.5 M Na_2SO_4	-12.44 ± 0.17	1.84 ± 0.05	-12.39 ± 1.6	1.09 ± 0.12	0.63 ± 0.07	1.72 ± 0.14	139.31 ± 18	0.017 ± 0.09

[a] Data are for the Ser14Ala variant at 10 °C. The $\Delta G°$ values are extrapolated to zero denaturant and a 1 M standard state peptide concentration. Kinetic rates listed are values extrapolated to zero denaturant and a 11 μM peptide concentration.

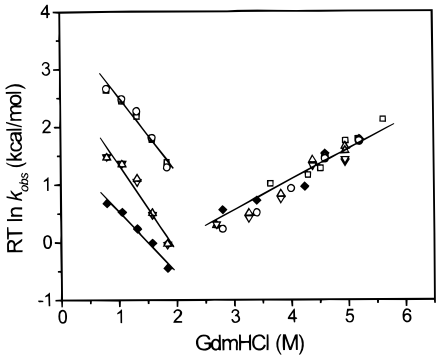

FIGURE 2: Folding and unfolding kinetics in cosolvents. Denaturant dependence of the apparent folding rates (left limb) and unfolding rates (right limb) of the Ser14Ala variant of GCN4-p1′ followed by fluorescence in 20 mM sodium acetate at pH 5.5 and 10 °C (◆), and in the presence of 5% TFE (○), 5% MetOH (△), 5% EtOH (▽), and 0.5 M sodium sulfate (□). The measured bimolecular folding rates (k_{obs} = [protein]k_f) have been scaled to conform to a uniform 5.5 μM protein concentration.

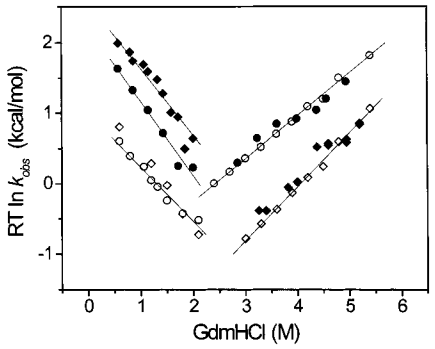

FIGURE 3: Ala to Gly mutagenesis in 5% TFE. Kinetics of the folding reactions of the Ser14Ala (◇ and ◆) and Ser14Gly (○ and ●) variants of GCN4-p1′ in the presence of 0 (white symbols) and 5% TFE (black symbols), as followed by fluorescence in 20 mM sodium acetate at pH 5.5 and 10 °C. The measured bimolecular folding rates (k_{obs} = [protein]k_f) have been scaled to conform to a uniform 2 μM protein concentration.

$k_f^{H_2O}$) and $m° = m_u - m_f$, derived from eqs 1 and 6. Table 1 shows values determined for GCN4-p1′ under the conditions used here. The equivalence of $\Delta G°$ and $m°$ values from equilibrium measurements with the values determined independently from kinetic experiments demonstrates the applicability of a two-state model for GCN4-p1′ folding under all measured solvent conditions. This also confirms the validity of the fluorescence probe for measuring folding rates, since every probe measures the same rate in an all-or-none, two-state reaction.

The two-state nature of the folding pathway of GCN4-p1′ with and without alcoholic cosolvents allows us to characterize the transition state of these reactions, providing insight into the intrinsic nature of the folding of this coiled coil, as well as into the way in which monohydric alcohols affect it. In the presence of all the cosolvents, the unfolding activation energies, $\Delta G_u^‡$, remain essentially unchanged (Figures 2 and 3). The decrease in the folding activation energies, $\Delta G_f^‡$, accounts for the entire stabilizing effect of the cosolvents and is fully realized by the transition state (Figure 4). Hence, both the transition state and the native state are stabilized to the same extent by the cosolvents, even though only about 50% of the GdmHCl-sensitive surface area is buried in the transition state ($m_f/m° \approx 0.5$).

In analogy with the protein engineering Φ analysis conducted with amino acid substitutions (*23*, *26*), the degree of interaction of the cosolvent with the transition state relative to that with the native state can be quantified with a parameter $\Phi_f^{solvent}$. This parameter is given by the change in folding rate, $\Delta\Delta G_f^‡$ (displacement of the folding limb of the chevron) divided by the change in dimer stability, $\Delta\Delta G°$ (difference between the folding and unfolding displacements), upon addition of cosolvent. For all the cosolvents, the folding arm of the chevron is shifted upward by an amount equal to the change in stability while the position of the unfolding arm remains unchanged. Hence, the $\Phi_f^{solvent}$

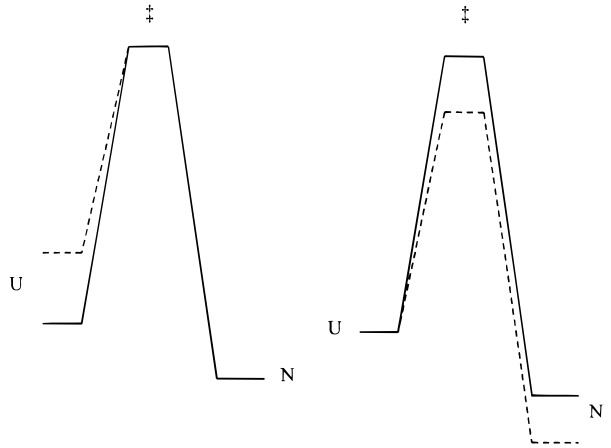

FIGURE 4: Reaction coordinate diagrams describing the mechanism of helix induction in buffer (solid lines) and perturbing amounts of cosolvents (dashed lines). The two diagrams are thermodynamically equivalent, insofar as they are both consistent with the equilibrium and kinetic effects of the cosolvents on GCN4-p1′. However, only the diagram on the left is consistent with the full helicity of the native state (N) and the absence of a substantial helical structure in the transition state (‡), since these cosolvents, and TFE in particular, cannot interact equivalently with these structurally different species.

values, describing the degree of energetic interaction of the transition state with the perturbation imposed on it, are essentially equal to 1 for each cosolvent.

Since TFE is thought to promote helix formation, the $\Phi_f^{solvent}$ value of 1 would seem to indicate that the transition state is fully helical. However, previous studies indicate that minimal helix is formed in the transition state of GCN4-p1′ folding, as indicated by an insensitivity of folding rates to Gly to Ala substitutions down the length of the coiled coil [$\Phi_f^{Ala-Gly} = 0.06-0.36$ (*15*)]. To test whether the presence of 5% TFE significantly alters the folding pathway, the Ala to Gly mutagenesis experiment is repeated in the presence of TFE at the solvent-exposed Ser14 position located at the center of the coiled coil (Figure 3). The folding rates of the alanine and glycine variants increased in TFE, but remained similar to each other with the $\Phi_f^{Ala-Gly}$ increasing only slightly from 0.14 to 0.18. Thus, the central position of the coiled coil remains largely unstructured in the transition state in 5% TFE. Further, a simultaneous triple Gly to Ala comparison (D7G/S14G/A24G vs D7A/S14A/A24, total of six substitutions in the dimer) in the presence of 5% TFE has a net $\Phi_f^{3\times Ala-3\times Gly}$ of ≈0.4, again confirming that a predominant portion of the transition state is nonhelical (L. Moran, J. Schneider, A. Kentsis, and T. R. Sosnick, unpublished results). Although the majority of the transition state is nonhelical, its interaction with TFE is fully realized. In this fashion, the stabilizing effect of TFE is at least partially divorced from helix formation in the transition state of this folding reaction.

Effect of TFE on Hydrogen Bonding. The effect of TFE on hydrogen bond strength is examined by measuring the change in coiled coil stability upon deuterium to protium amide substitution. In proteins, hydrogen isotope partitioning reflects the strength of the hydrogen bond (*16*−*18*; see the Discussion). Because the change in stability due to deuterium to protium substitution is small compared to the global free energy change for folding, the D−H exchange was carried out at the midpoint of the folding transition, K_d, where minimal changes in stability elicit maximal changes in signal. For example, a measurable 2% change in CD signal equates to a 5 cal/mol change in coiled coil stability, or approximately 80 mcal/mol for each of the 60 hydrogen bonds in the coiled coil. Cosolvent addition decreases the K_d by up to 20-fold, and so we could conduct the experiment at the K_d value appropriate for each solvent condition, the protein concentration was reduced accordingly. Concentration-dependent unfolding measurements are taken in 0 and 5% TFE and 0.5 M sodium sulfate to determine K_d values (data not shown), while values in 2.5 and 10% TFE are obtained by extrapolation.

To compare only the effect of D−H amide substitution on stability, and not changes associated with a difference in bulk solvent, fully denatured and deuterated protein is manually diluted 100-fold into H_2O solvent under conditions where stability could be measured prior to significant amide isotopic exchange. At pH 4.55 and 10 °C, half of the molecules fold within seconds and equilibrate to the new solvent condition; however, amide hydrogen exchange takes minutes (*27*) [side chain hydrogens become protonated in seconds (*21*) and do not contribute to the measured change in stability]. Hence, the stability of the species with a fully deuterated backbone, ΔG_D°, in bulk H_2O is determined from the initial Θ_{222} reading, and the stability of the molecule with a fully protonated backbone, ΔG_H°, is measured after amide exchange is complete. The difference, $\Delta\Delta G_{D-H}^\circ$ ($=\Delta G_H^\circ - \Delta G_D^\circ$), reflects only the change in protein stability due to backbone protonation since both measurements are taken under the same solvent conditions. The modulation of $\Delta\Delta G_{D-H}^\circ$ by 5% TFE serves to identify whether it preferentially strengthens or weakens helical hydrogen bonds, as compared to those to water. A greater $\Delta\Delta G_{D-H}^\circ$ in the presence of TFE indicates a strengthening of intramolecular hydrogen bonds, while a decrease in the energetic preference for protium indicates their weakening.

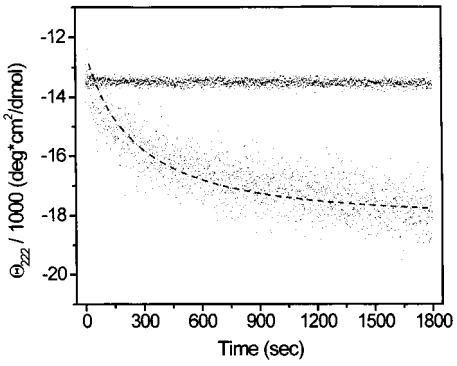

FIGURE 5: Kinetics of the change in stability upon D−H amide isotopic exchange obtained by monitoring CD at 222 nm. This experiment was carried out at the midpoint of the dimerization folding transition in the absence (bottom trace) and presence (top trace) of 5% TFE in 20 mM sodium acetate at pH 4.55 and 10 °C. The dashed line represents the predicted kinetic behavior calculated as a sum of the individual decays of each amide proton having an exchange protection factor of 2, as expected for a population composed of 50% unfolded molecules.

The time course of hydrogen exchange of fully deuterated protein with and without 5% TFE is shown in Figure 5. These experiments are conducted with a monomeric Ala24Gly substituted version of the coiled coil, GCN4-p2′, which has an additional amino-terminal Cys-Gly-Gly disulfide-bonded cross-link. This disulfide cross-link is reduced with phosphine to produce a dimeric species whose stability was equal to that of a tetherless version (R. P. Bhattacharyya and T. R. Sosnick, unpublished results). Upon injection, fully deuterated GCN4-p2′ recovers approximately 40% of its native ellipticity. Complete hydrogen exchange takes approximately 20 min and increases the molar ellipticity by about 15%, equivalent to 237 ± 29 cal/mol or about 4 ± 0.5 cal/mol for each of the ∼60 hydrogen bonds in the coiled coil. The presence of 2.5 (0.37 M) and 5% TFE (0.74 M) reduces the net isotope effect on coiled coil stability to 93 and 20 cal/mol, respectively, with a nearly linear dependence upon TFE concentration (Figure 6). Surprisingly, the energetic preference for protons, and thus hydrogen bond strength, is decreased in the presence of TFE, indicating that the mode of helix induction by TFE is not dependent on the strengthening of native helical hydrogen bonds.

The intrinsic rate of hydrogen exchange of individual solvent-exposed amide deuterons is sequence-dependent and is spread between 0.0781 and 0.599 min^{-1} at pH 4.55 and 10 °C (*21*). The observed exchange rates are slowed by a protection factor, PF, the fraction of time the amide deuterons are in an exchange-competent state (*28*). In these experi-

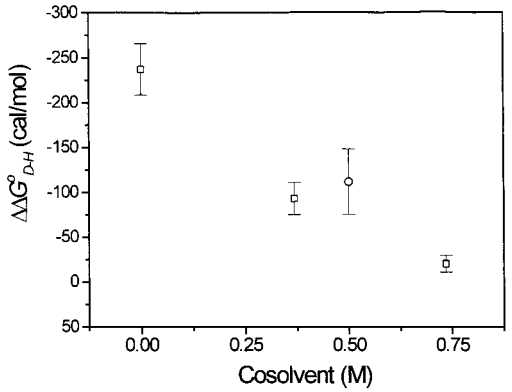

FIGURE 6: Changes in stability upon D−H amide exchange in the presence of TFE (□) and sodium sulfate (○) as a function of cosolvent concentration.

ments conducted at the denaturation midpoint, this fraction is 50% and PF = 1 + $K_U \approx 2$. The predicted HX time course, constituted by the sum of the individual exponential decays of each amide having a PF equal to 2, and the observed data are shown in Figure 5. The predicted time course agrees with the observed data to within 15%, possibly reflecting a slight inaccuracy in the calculation of intrinsic HX rates, or in the conduct of the experiment at the precise midpoint of the concentration folding transition.

Transition State and Hydrogen Bond Strength. Having characterized the transition state of GCN4-p1′ in terms of its interaction with monohydric alcohols, we sought to examine hydrogen bond strength in the transition state by measuring the effect of amide hydrogen isotope substitution on the folding kinetics of the wild-type GCN4-p1′. Just as there exists a difference in strength between amide-to-carbonyl hydrogen bonds in the folded state and amide-to-water hydrogen bonds in the unfolded state, as shown above by the increase in stability upon D−H substitution, $\Delta\Delta G^{\circ}_{D-H}$, the relative effect of D−H substitution on folding kinetics, can be used to determine hydrogen bond strength in the folding transition state. To eliminate any possible bulk solvent effects, these kinetic measurements for both the deuterated and protonated forms are taken under identical 12% D_2O solvent conditions. Although the equilibrium isotope effect discussed above was measured in the absence of guanidine, the kinetic measurements are taken in varying guanidine concentrations. However, since the dependence of refolding and unfolding rates on guanidine concentration, quantified by m_f and m_u, respectively, are equal in deuterated and protonated forms of the protein, guanidine fails to perturb the effect of isotope substitution.

As can be seen from Figure 7, the refolding activation energy, $\Delta G^{\ddagger}_f$, remains unchanged in response to D−H amide substitution. The difference in activation energy, $\Delta\Delta G_f^{\ddagger D-H}$, is −10 ± 4 cal/mol and within the scatter of the data about the least-squares fitted line. The effect of amide isotope substitution on folding, parametrized as $\Phi_f^{D-H} = \Delta\Delta G_f^{\ddagger D-H}/\Delta\Delta G^{\circ}_{D-H}$, is essentially zero. Although the effect of D−H substitution is small ($\Delta\Delta G^{\circ}_{D-H}$ = 182 ± 5 cal/mol) compared to the effect of mutations ordinarily observed in Φ analysis, it is nevertheless significant and reproducible. Moreover, the kinetically determined value for the change in equilibrium stability upon isotope substitution fully recapitulates the value from separate equilibrium measurements at the midpoint of the GdmHCl folding transition ($\Delta\Delta G^{\ddagger}_u - \Delta\Delta G^{\ddagger}_f$ = 179 ± 7, $\Delta\Delta G^{\circ}_{D-H}$ = 182 ± 5 cal/mol; Figure 7 inset). Moreover, an analogous experiment using a cross-linked GCN4-p2′, in which the transition state contains a substantial amount of helical structure, yielded a Φ_f^{D-H} of ≈0.6 (L. Moran, J. Schneider, A. Kentsis, and T. R. Sosnick, unpublished results). The expression of the D−H isotope effect on the unfolding rates indicates that the energetic preference of deuterium to protium substitution is nearly equal in both the unfolded and transition states. This means that the average strength of the hydrogen bonds in the transition state is nearly equal to the strength of those present in the unfolded state.

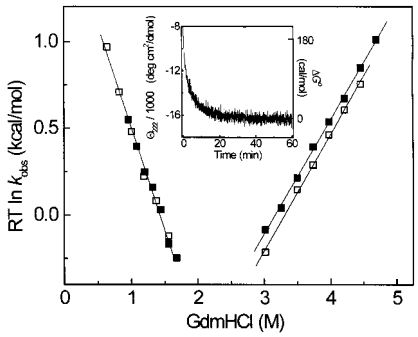

FIGURE 7: Denaturant dependence of the folding rates of wild-type GCN4-p1′ in fully protonated (□) and fully deuterated (■) states, as measured using fluorescence spectroscopy in 20 mM sodium acetate at pH 4.55 and 10 °C and 12% (v/v) D_2O. The measured bimolecular refolding rates have been scaled to values corresponding to a 5.5 μM protein concentration. In the inset is depicted the change in equilibrium stability of GCN4-p1′ upon backbone D−H substitution, as monitored using CD at 222 nm and carried out at the midpoint of the GdmHCl denaturation transition under solvent conditions identical to those in the kinetic experiment. Kinetically and thermodynamically determined values for the effect of amide hydrogen isotope substitution on coiled coil stability ($\Delta\Delta G^{\circ}_{D-H}$) are equal.

Similar folding measurements have been attempted before, but failed to reveal any significant differences in folding between deuterated and protonated proteins (*29*, *30*). Potentially, this was due to a slight inequality in the bulk solvent conditions (0 vs 9% D_2O; *30*), which may have masked the small effect of amide isotope substitution, as it did with GCN4-p1′ (data not shown). Itzhaki and Evans, on the other hand, utilized identical bulk solvent conditions (*29*), but may have failed to observe the effect of amide D−H substitution, having monitored only the refolding kinetics.

DISCUSSION

TFE's Stabilization of Nonhelical Structure. The original goal of this study was to quantify the total helicity of the folding transition state by studying the effects of low concentrations of TFE on the folding kinetics of GCN4-p1′. If the helix-inducing effect of TFE is mediated through the stabilization of features thought to be important for α-helix stability, e.g., helical backbone geometry and *i*, *i* + 4 hydrogen bonds, the enhancement of the folding rates relative to the change in equilibrium stability should quantify the net helical content of the transition state. The presence of 5% TFE increased the stability of the coiled coil 20-fold and accelerated the rate of folding to the same degree. Thus, the energetic interaction of TFE with the transition state is

equivalent to TFE's interaction with the native state (Figure 2). This would seem to imply that the transition state is fully helical.

However, previous studies indicated that minimal helix is present in the transition state (*15*). Refolding rates were largely unchanged when helix-stabilizing mutations (Gly to Ala) were introduced at solvent-exposed positions. The possibility is negated that even at these low concentrations, TFE could alter the folding pathway so drastically as to change the character of the transition state to be nearly 100% helical, this being the relative effect of TFE on the folding transition state. The Gly to Ala comparison is repeated in 5% TFE at the Ser14 position in the center of the coiled coil, and the folding rates of both species remain very similar, indicating that helical structure is still largely absent at the center Ser14 position ($\Phi_f^{Ala-Gly} = 0.18$). Furthermore, a triple site Gly to Ala comparison (D7G/S14G/A24G vs D7A/S14A/A24) in the presence of 5% TFE has a net $\Phi_f^{3\times Ala-3\times Gly}$ of ≈0.4 (L. Moran, J. Schneider, A. Kentsis, and T. R. Sosnick, unpublished results). Although the translation of this fractional Φ value into a precise helical percentage is difficult, it is clear that the net helical content in the transition state is less than 50%. However, TFE stabilizes the transition state to the same extent (i.e., ≈100%) as the helical native state. Hence, TFE's secondary structure-inducing effect can be divorced from helix formation.

TFE's Effect on Hydrogen Bond Strength. Although formation of intramolecular hydrogen bonds occurs during helix formation and is considered to be an integral contributor to the energetics of the reaction, TFE's helix-inducing ability is not due to the explicit strengthening of helical hydrogen bonds. In the presence of 5% TFE, the change in stability of the coiled coil during amide D−H substitution decreases by 217 cal/mol. The equilibrium D−H isotope effect in proteins reflects the energetic preference of stronger hydrogen bonds for protium (*16*−*18*). Fractionation factors, the average fractional occupancy of D in the bond relative to that in the bulk solvent, are >1 for strong, short (low-barrier) hydrogen bonds and for weak, long (high-barrier) hydrogen bonds, whereas intermediate-strength hydrogen bonds tend to have factors of <1 (*31*, and references therein). This pattern of isotopic fractionation is due to the greater zero point vibrational energy of the lower-mass protons. In the high-barrier limit, both isotopes predominantly reside in a single energy well on the donor so that the deuteron's lower zero-point energy makes it the preferred isotope. In the low-barrier limit, the hydrogen atom resides at an energy above the barrier and is shared nearly equally between the donor and acceptor. Effectively, the atom resides in a single well, so again the deuteron is preferred. However, for intermediate-barrier heights, the deuteron's lower energy leads to a more differential occupancy of the donor and acceptor sites, while the proton's partitioning between these sites is more uniform due to its higher vibrational energy. The proton's more uniform partitioning increases the covalent character of the bond. This results in an increased stabilization and a net preference for protium in the intermediate-barrier regime.

Since low-barrier hydrogen bonds have rarely been observed in proteins (*32*), and amide−carbonyl hydrogen bonds are longer than 2.5 Å (*33*), protein hydrogen bonds exist in the high- to intermediate-barrier limit and have an average fractionation factor of 0.9 ± 0.1 (*17*, *18*). Similarly, fractionation factors for most low-molecular weight carboxylates, amines, and amides are also close to unity (*34*). In the weak- to intermediate-barrier limit applicable to proteins, stronger hydrogen bonds accumulate protium relative to deuterium. Hence, a preferential partitioning of protons into intramolecular hydrogen bonds in proteins indicates a strengthening of these amide−carbonyl connectivities, while preferential partitioning of D indicates their weakening.

Replacement of deuterium with protium at the amide positions of the coiled coil leads to a stabilization of 237 cal/mol in the absence of TFE, which is reduced to 20 cal/mol by the addition of 5% TFE. Thus, the energetic preference for protium in the amide−carbonyl hydrogen bonds (relative to amide−water hydrogen bonds) in the coiled coil is rendered smaller by TFE. As a result, TFE has a weakening effect on helical hydrogen bond strength. This is quite surprising as hydrogen bonding is considered to be an integral structural and energetic factor in helix formation, as well as in the substrate for the mechanism of helix induction by TFE. It is interesting that the energetic preference of protium for an amide−carbonyl hydrogen bond relative to an amide−water hydrogen bond indicates that the former is the stronger of the two bonds.

Mechanism of Helix Induction by TFE. Surprisingly, 5% TFE imparts 1.7 kcal/mol of stability to this fully α-helical homodimer, but does not increase intramolecular hydrogen bond strength. These observations can be made coherent by considering that in addition to hydrogen bond formation, the polypeptide chain undergoes considerable desolvation in forming an α-helix (*35*). TFE's effect on coiled coil folding may be explained by its solvent-structuring properties, which promote burial of hydrogen bonding moieties, particularly amides and carbonyls.

The equivalent interaction of monohydric alcohols with the transition and native states can yield two equivalent thermodynamic reaction coordinates. The transition and native states are equally stabilized by TFE, or its effect is manifested through the destabilization of the unfolded state (Figure 4). Since the transition and native states are considerably different in terms of their helical content (less than 50% vs ≈100% helical) and their extents of guanidine-sensitive surface burial ($m_f/m^\circ \approx 0.5$), it is unlikely that TFE can interact equivalently with both. Thus, the model in which monohydric alcohols act on the unfolded species is most commensurate with both structural and thermodynamic data. According to this scenario, perturbing amounts of TFE stabilize GCN4-p1′ and accelerate its refolding by destabilizing the unfolded state.

In consonance with the three decade-old proposal of Brighetti and colleagues, who noted anomalous thermodynamic properties of water−alcohol solutions (*12*), we believe that the helical enhancement by monohydric alcohols is caused by the decrease in the extent of backbone solvation in the unfolded state rather than by the explicit stabilization of hydrogen bonds. Kemp and co-workers examined the interconversion of helical and nonhelical acetamido conformers and also concluded that TFE's stabilization of the intramolecularly hydrogen bonding conformer is accomplished by the preferential destabilization of solvent-exposed amides and carbonyls (*14*).

Alcohols as Kosmotropes. As seen with TFE, the energetic interactions of 5% MetOH, 5% EtOH, and 0.5 M sodium sulfate are fully realized in the folding transition state and have an essentially unitary $\Phi_f^{solvent}$ value. Regarding the question of how monohydric alcohols destabilize the unfolded species, TFE's mimicry by 0.5 M sodium sulfate is quite illuminating. Sulfate salts rank high in the Hofmeister series and are potent kosmotropes (*36*, *37*), acting by increasing the stability of the structure of bulk water (*38*), its surface tension (*39*), and the entropy of solute dehydration. As a consequence, the energy required by the polypeptide chain to unfold, and thereby increase the dimensions of its solvent cavity, increases. The free energy of this cavity formation represents a major contributor to the stabilization of proteins by kosmotropic salts (*40*). Although as a class, the water-structuring kosmotropes destabilize the unfolded state, their specific chemical properties may determine whether they primarily interfere with backbone desolvation or apolar exposure (e.g., aliphatic side chains). For a comprehensive review, see ref *41*.

To define the mechanism of helix induction by TFE observed in this work in terms of its effect on solvent structure, monohydric alcohols appear to act in a kosmotropic fashion to destabilize the more hydrated unfolded state. NMR observation of the helix-stabilizing effect of TFE also shows that it is not due to a direct interaction of the cosolvent with the polypeptide, but is rather strictly thermodynamic in origin (*13*). Furthermore, the helix-inducing effect of TFE does not involve stabilization of electrostatic interactions due to the dielectric properties of aqueous TFE solutions (*2*). The kosmotropic effect of monohydric alcohols is evident only at relatively low concentrations, where solvent structure is perturbed, but not disrupted. At higher concentrations, particularly above 40%, the composition of the solvent becomes less like bulk water and more like bulk alcohol. In the latter regime, the helix-inducing ability of TFE plateaus (*14*, *42*), and the presence of the hydrophobic trifluoroethyl surface begins to promote hydrophobic side chain exposure and destabilize tertiary architectures (*43*). At concentrations of >20%, TFE has been recently proposed to stabilize helices by disordering the local hydration shell around the helical state in a chaotropic manner (*44*).

The solvent-structuring effect of TFE is partially rationalized by its physicochemical properties. TFE is more acidic than water, having a pK_a of 12.4 (*45*). Symons proposed that the increased acidity and decreased basicity of alcohols may act to decrease the fraction of water molecules which have nonbonded lone pairs, as observed using infrared and NMR spectroscopies (*46*). By increasing the fraction of these so-called Symons defects, TFE makes water less hydrogen bond-competent which promotes desolvation of polypeptide functionalities such as amides and carbonyls which interact with water. In light of the water-structuring mechanism of helix induction by TFE, it is interesting to note that alcohols lead to large negative entropy changes upon mixing with water. Furthermore, only alcohols and some aliphatic amines (*47*) have been observed to maintain water cohesion and raise the temperature of the maximum density of water (*48*). Thus, in addition to the data presented in this work, a considerable body of evidence supports the conclusion that the presence of low concentrations of monohydric alcohols has a structuring effect on the binary alcohol−water solvent, particularly with respect to the solvation of the hydrophilic polypeptide backbone.

The kosmotropic model of the interaction of monohydric alcohols with proteins is capable of explaining a puzzling aspect of the thermal helix−coil transitions in TFE. In the work of Luo and Baldwin (*42*), the mean helix propensity is observed to increase with increasing TFE concentrations, yet $\Delta H°$ of the coil−helix transition is seen to decrease. Luo and Baldwin suggest that one reason for this may be a "preferential interaction with TFE relative to H_2O between the helix versus the coil forms of the peptide", consistent with our interpretation that aqueous TFE solvent preferentially destabilizes the unfolded state.

Transition State Hydrogen Bonds. From the current studies, the transition state of the coiled coil is seen to be completely desolvated with respect to its alcohol-sensitive surface area ($\Phi_f^{solvent} \approx 1$), probably comprised of the backbone amide and carbonyl groups. However, the minor sensitivity of refolding rates to Ala to Gly substitution in 5% TFE, both for the single-site (this work) and double- and triple-site substitutions (L. Moran, J. Schneider, A. Kentsis, and T. R. Sosnick, unpublished results), indicates that the major fraction of helical structure is absent in the transition state. Uncertainty in the interpretation of fractional Φ values, particularly for alanine versus glycine comparisons which specifically probe backbone conformational entropy rather than helical structure per se, precludes quantification of the total amount of helix. However, the small effect of amide hydrogen isotope substitution on the refolding kinetics ($\Phi_f^{D-H} \approx 0$) indicates that amide hydrogen bonds in the unfolded and transition states are of nearly equal strength, and both are weaker than those in the native state.

Since the transition state exists as a desolvated species, amides and carbonyl moieties are probably not interacting with bulk solvent. With respect to the identity of the hydrogen bonding partners in the transition state, the majority of the backbone either forms nonhelical intramolecular bonds or bonds to water molecules in a solvation shell. In the latter scenario, the protein becomes desolvated during refolding with respect to bulk solvent, but remains hydrogen bonded to water molecules in a solvation layer. Although these two possibilities for the structural identity of transition state hydrogen bonds remain equivocal in this study, transition state hydrogen bonds are weaker than those in the native state.

Features of the Folding Transition State. We find it difficult to synthesize a simple structural picture of the transition state in light of the current data. The difficulty comes from the conclusion that the transition state must be a desolvated species with respect to its alcohol-sensitive surface area (polypeptide backbone; $\Phi_f^{solvent} = 1$) while still possessing minimal (e.g., $\Phi_f^{Ala-Gly}{}_{Ser14} = 0.14$), but not necessarily zero, helical content. Additionally, this species buries only half of its guanidine-sensitive surface area (side chains and backbone; $m_f/m° \approx 0.5$) and lacks native strength hydrogen bonds ($\Phi_f^{D-H} \approx 0$). Two delimiting structural models are possible. (1) The above four features of the transition state have an exact correspondence to underlying structure, thereby making the transition state truly desolvated with respect to its backbone amide and carbonyl groups, and

constrained in such a way as to satisfy intramolecular hydrogen bonds without forming large quantities of helical structure. (2) The transition state appears to be desolvated insofar as it does not interact with TFE, but is surrounded by a nonbulk hydration shell that hydrogen bonds with the polypeptide. This gives rise to non-native strength hydrogen bonds, and allows the protein to fluctuate in a nonhelical fashion. Notwithstanding the exact nature of the small $\Phi_f^{Ala-Gly}$ and Φ_f^{D-H} values, the formation of helical structure and native-like hydrogen bonds is not the major component of the folding coordinate.

The more cardinal dimension is backbone burial, as evidenced by the $\Phi_f^{solvent}$ value of near unity for TFE. Thus, the energetically uphill search for the transition state (*49*) is achieved by dehydrating the protein backbone while only burying half of the total guanidine-sensitive surface area. The transition state is achieved without the formation of native strength hydrogen bonds. Instead, these become strengthened only on the native side of the folding barrier, consistent with late formation of the majority of the helical structure.

Bolen and co-workers recently emphasized that naturally occurring osmolytes such as trimethylamine *N*-oxide (TMAO) stabilize proteins by raising the energy associated with solvating the polypeptide backbone in the unfolded state rather than directly stabilizing the folded state (*50*, *51*), just like the scenario proposed here for TFE. Furthermore, only monohydric alcohols and aliphatic amines such as TMAO have been observed to raise the temperature of the maximum density of water, indicative of its structuring (*47*). These unique common features suggest that the mechanism of protein stabilization by various osmolytes and monohydric alcohols is likely to be similar.

Recently, Rose and colleagues proposed that local structure in the unfolded state restricts the conformational search for the transition state, thereby guiding folding (*52*). The implications of this proposal are quite intriguing, as the concept of a polypeptide chain being productively guided through a vast conformational space via the formation of predisposed local interactions is easily imaginable and quite cogent. The presence of TMAO results in compaction of the unfolded protein (*51*) which, according to this view, would induce the folding of predisposed segments in a hierarchical manner. However, an alternative perspective is that TFE and osmolytes (*50*, *51*) exert their counterdenaturant effects by way of affecting global polypeptide solvation, and not the stability of local folding interactions. In the case of the coiled coil, the latter mechanism appears to be in effect as extensive α-helical structure and even native-like hydrogen bonds form late. Backbone conformational biases can exist in the unfolded state. But, as long as they exist in the transition state to the same degree, no effect on refolding rates would be observed. Whether or not significant local structural predispositions exist, the search for the folding transition state of the structurally uncomplicated coiled coil proceeds with comprehensive bulk desolvation of the polypeptide backbone.

ACKNOWLEDGMENT

We thank W. F. DeGrado, S. W. Englander, L. B. Moran, L. Mayne, R. P. Bhattacharyya, M. A. Weiss, J. Schneider, D. Baker, N. Kallenbach, G. Rose, D. W. Bolen, R. L. Baldwin, T. Pan, and J. Piccirilli for numerous enjoyable and enlightening discussions; S. Jackson and R. Wilk for generously providing synthesized peptides; and L. B. Moran, R. P. Bhattacharyya, M. Makinen, W. F. DeGrado, N. Kallenbach, and S. W. Englander for comments on the manuscript.

REFERENCES

1. Sancho, J., Neira, J. L., and Fersht, A. R. (1992) *J. Mol. Biol. 224*, 749−58.
2. Nelson, J. W., and Kallenbach, N. R. (1986) *Proteins 1*, 211−7.
3. Jasanoff, A., and Fersht, A. R. (1994) *Biochemistry 33*, 2129−35.
4. Schonbrunner, N., Wey, J., Engels, J., Georg, H., and Kiefhaber, T. (1996) *J. Mol. Biol. 260*, 432−45.
5. Hamada, D., and Goto, Y. (1997) *J. Mol. Biol. 269*, 479−87.
6. Lu, H., Buck, M., Radford, S. E., and Dobson, C. M. (1997) *J. Mol. Biol. 265*, 112−7.
7. Buck, M., Schwalbe, H., and Dobson, C. M. (1995) *Biochemistry 34*, 13219−32.
8. Shiraki, K., Nishikawa, K., and Goto, Y. (1995) *J. Mol. Biol. 245*, 180−94.
9. Tung, C. H., and Ji, H. F. (1995) *J. Phys. Chem. 99*, 8311−6.
10. Bodkin, M. J., and Goodfellow, J. M. (1996) *Biopolymers 39*, 43−50.
11. Rajan, R., and Balaram, P. (1996) *Int. J. Pept. Protein Res. 48*, 328−36.
12. Conio, G., Patrone, E., and Brighetti, S. (1970) *J. Biol. Chem. 245*, 3335−40.
13. Storrs, R. W., Truckses, D., and Wemmer, D. E. (1992) *Biopolymers 32*, 1695−702.
14. Cammers-Goodwin, A., Allen, T. J., Oslick, S. L., McClure, K. F., Lee, J. H., and Kemp, D. S. (1996) *J. Am. Chem. Soc. 118*, 3082−90.
15. Sosnick, T. R., Jackson, S., Wilk, R. M., Englander, S. W., and DeGrado, W. F. (1996) *Proteins 24*, 427−32.
16. Kreevoy, M. M., and Liang, T. M. (1980) *J. Am. Chem. Soc. 102*, 3315−22.
17. Loh, S. N., and Markley, J. L. (1994) *Biochemistry 33*, 1029−36.
18. Bowers, P. M., and Klevit, R. E. (1996) *Nat. Struct. Biol. 3*, 522−31.
19. Choma, C. T., Lear, J. D., Nelson, M. J., Dutton, L. P., Robertson, D. E., and DeGrado, W. F. (1994) *J. Am. Chem. Soc. 116*, 856−65.
20. Pace, C. N., Vajdos, F., Fee, L., Grimsley, G., and Gray, T. (1995) *Protein Sci. 4*, 2411−23.
21. Bai, Y., Milne, J. S., Mayne, L., and Englander, S. W. (1993) *Proteins 17*, 75−86.
22. Zitzewitz, J. A., Bilsel, O., Luo, J., Jones, B. E., and Matthews, C. R. (1995) *Biochemistry 34*, 12812−9.
23. Matthews, C. R. (1987) *Methods Enzymol. 154*, 498−511.
24. Jackson, S. E., and Fersht, A. R. (1991) *Biochemistry 30*, 10428−35.
25. Pace, C. N. (1975) *CRC Crit. Rev. Biochem. 3*, 1−43.
26. Fersht, A. R., Matouschek, A., and Serrano, L. (1992) *J. Mol. Biol. 224*, 771−82.
27. Connelly, G. P., Bai, Y., Jeng, M.-F., Mayne, L., and Englander, S. W. (1993) *Proteins 17*, 87−92.
28. Englander, S. W., and Kallenbach, N. R. (1984) *Q. Rev. Biophys. 16*, 521−655.
29. Itzhaki, L. S., and Evans, P. A. (1996) *Protein Sci. 5*, 140−6.
30. Parker, M. J., and Clarke, A. R. (1997) *Biochemistry 36*, 5786−94.
31. Hibbert, F., and Emsley, J. (1990) *Adv. Phys. Org. Chem. 26*, 255−379.
32. Ash, E. L., Sudmeier, J. L., De Fabo, E. C., and Bachovchin, W. W. (1997) *Science 278*, 1128−32.
33. Ichikawa, M. (1978) *Chem. Phys. Lett. 79*, 583.
34. Schowen, R. L. (1972) *Prog. Phys. Org. Chem. 9*, 197.

35. Honig, B., and Yang, A. S. (1995) *Adv. Protein Chem. 46*, 27−58.
36. Baldwin, R. L. (1996) *Biophys. J. 71*, 2056−63.
37. Cacace, M. G., Landau, E. M., and Ramsden, J. J. (1997) *Q. Rev. Biophys. 30*, 241−77.
38. Collins, K. D., and Washabaugh, M. W. (1985) *Q. Rev. Biophys. 18*, 323−422.
39. Melander, W. R., Corradini, D., and Horvath, C. (1984) *J. Chromatogr. 317*, 67−85.
40. Kestner, N. R., and Sinanoglu, O. (1965) *Discuss. Faraday Soc. 40*, 266−7.
41. Timasheff, S. N. (1995) *Methods Mol. Biol. 40*, 253−69.
42. Luo, P., and Baldwin, R. L. (1997) *Biochemistry 36*, 8413−21.
43. Monera, O. D., Zhou, N. E., Kay, C. M., and Hodges, R. S. (1993) *J. Biol. Chem. 268*, 19218−27.
44. Walgers, R., Lee, T. C., and Cammers-Goodwin, A. (1998) *J. Am. Chem. Soc. 120*, 5073−9.
45. Murto, J. (1964) *Acta Chem. Scand. 18*, 1043−53.
46. Symons, M. C. R. (1981) *Acc. Chem. Res. 14*, 179−87.
47. Franks, F., and Watson, B. (1967) *Trans. Faraday Soc. 63*, 362.
48. Franks, F., and Ives, D. J. G. (1966) *Q. Rev. Chem. Soc. 57*, 1.
49. Sosnick, T. R., Mayne, L., and Englander, S. W. (1996) *Proteins 24*, 413−26.
50. Wang, A., and Bolen, D. W. (1997) *Biochemistry 36*, 9101−8.
51. Qu, Y., Bolen, C. L., and Bolen, D. W. (1998) *Proc. Natl. Acad. Sci. U.S.A.* (in press).
52. Aurora, R., Creamer, T. P., Srinivasan, R., and Rose, G. D. (1997) *J. Biol. Chem. 272*, 1413−6.

BI981641Y